

cross-correlates it with the original particle. For $n=5$, 6, and 7, the 90 most n -fold-symmetric particles were picked, aligned, and averaged, albeit without applying any symmetry. Insets a–c in Fig. 5 show these averages for the full-length Vps4p images. By visual inspection, even the most 5- and 7-fold-like particles produced averages that appeared 6-fold symmetric. For a more quantitative comparison, the rotational power spectrum of each 5-, 6-, and 7-fold-like average was calculated. The only clear peak occurred in the spectra of the 6-fold-like average (data not shown). The same analysis for the most 5-fold-like or the most 7-fold-like particles showed only small signals, with 5- and 6-fold or 7- and 6-fold values displaying approximately equal magnitudes (not shown). Finally, the average rotational power spectrum of the combined set of all 270 particles picked for the 5-, 6-, and 7-fold-like averages was calculated, which showed a single strong peak corresponding to 6-fold symmetry (shown for the full-length Vps4p complex in Fig. 5). Similar results were obtained for the Δ N-Vps4p and Vta1p-Vps4p complexes (data not shown).

As a third independent method, the program RotaStat,⁷¹ which reports the relative likelihood of different symmetries within a set of images in different radial bands, was used. Applying RotaStat to the combined data set of 270 particles in Fig. 5a–c

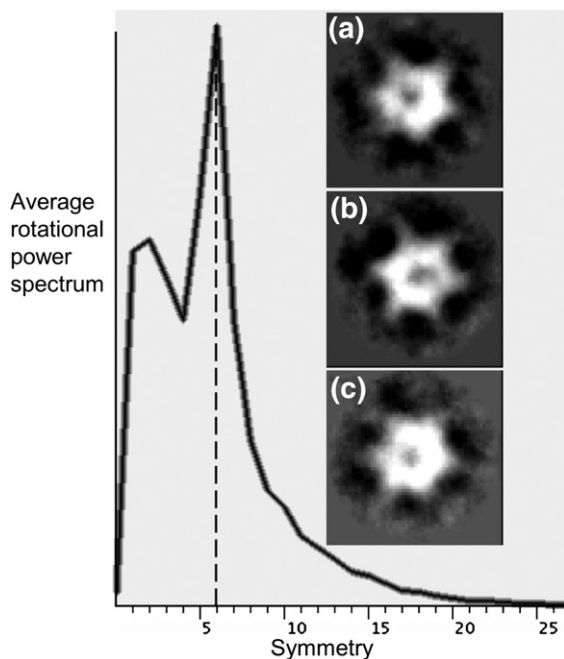


Fig. 5. Directed symmetry search. The EMAN program *startcsym* was used to search the particle gallery to find the images that were most apparently C_n -fold ($n=5, 6, 7$) symmetric. Three classes containing the 90 most 5-fold (a), 6-fold (b), and 7-fold (c) symmetric particles were aligned and averaged. Even the most 5- and 7-fold symmetric particles appear 6-fold symmetric. The averaged rotational power spectrum of all 270 particles is also shown, with a clear peak indicating 6-fold symmetry. Further statistical analysis by RotaStat also overwhelmingly favored 6-fold symmetry (not shown).

showed clearly that 6-fold symmetry was the most significant (the “spectral ratio product” was 33 orders of magnitude higher for C_6 symmetry than the next most likely symmetry). Similar results were obtained for the Δ N-Vps4p and Vta1p-Vps4p images. These three analyses demonstrate that, like most AAA proteins, Vps4p complexes are 6-fold symmetric; they also demonstrate that if any Vps4p particles assembled with either 5- or 7-fold symmetry in this analysis, their numbers were negligible.

Three-dimensional reconstructions

Three-dimensional reconstructions were generated from the images using standard “single-particle” methods and imposing 6-fold symmetry (see Fig. S2 for Euler angle distributions and Figs. S3–S5 for comparisons of final class averages and corresponding model projections for all three reconstructions). The Fourier shell correlation (FSC) curves are shown in Fig. S6, and the estimated resolutions (FSC=0.5) are 25, 34, and 38 Å for the Δ N-Vps4p, full-length Vps4p, and Vta1p-Vps4p complexes, respectively. The N-terminal region of Vps4p contains an MIT domain (residues 1–79), followed by a linker region that is poorly ordered in solution (residues 80–121).^{26,28,29} This region of the protein is therefore likely to be at least partially disordered in the reconstruction. The adaptor protein Vta1p consists of three regions—an N-terminal segment that binds Vps60p,^{10,31,32} a C-terminal Vta1/SBP1/LIP5 (VSL) domain that dimerizes and binds Vps4p,³⁰ and an intervening linker that is likely to be in a disordered or an extended conformation (W.I.S., unpublished data). Thus, the resolutions obtained for the different complexes correlate with the expected degree of disorder, although it is unclear what effect cross-linking may have had on domain flexibility, since intrinsically flexible domains could have been stabilized by cross-linking and their visibility in averages would depend on how uniform their (cross-linked) positions were. FSC analysis requires splitting a data set into halves and comparing the corresponding half-data-set reconstructions. To check whether the resolutions obtained were limited by particle numbers or heterogeneity, we further split the Vta1p-Vps4p data set into quarters and carried out four independent reconstructions. These reconstructions (Fig. S7) and their FSC curves show that the heterogeneity of the particles, rather than the total number of images included, is the principal resolution limitation.

Structures of Δ N-Vps4p, full-length Vps4p, and Vta1p-Vps4p complexes

As shown in Fig. 6, the Δ N-Vps4p, full-length Vps4p, and Vta1p-Vps4p complexes all display distinctive bowl-like structures with a central cavity in the upper half. The dimensions of the Vps4p assemblies match the double-hexameric ring structures of NSF⁴⁴ and ClpB⁴⁷ reconstructed by cryo-EM